Atmospheric Environment 45 (2011) 6048–6056

Contents lists available at ScienceDirect

Atmospheric Environment

journal homepage: www.elsevier.com/locate/atmosenv

Semi-continuous measurement of water-soluble ions in $PM_{2.5}$ in Jinan, China: Temporal variations and source apportionments

Xiaomei Gao [a], Lingxiao Yang [a,b,*], Shuhui Cheng [a], Rui Gao [a], Yang Zhou [a], Likun Xue [a], Youping Shou [a], Jing Wang [a], Xinfeng Wang [a], Wei Nie [a], Pengju Xu [a], Wenxing Wang [a,c]

[a] Environment Research Institute, Shandong University, Jinan 250100, China
[b] School of Environmental Science and Engineering, Shandong University, Jinan 250100, China
[c] Chinese Research Academy of Environmental Sciences, Beijing 100012, China

ARTICLE INFO

Article history:
Received 18 April 2011
Received in revised form
21 July 2011
Accepted 24 July 2011

Keywords:
semi-continuous
Water-soluble ions
$PM_{2.5}$
Seasonal and diurnal variations
Transport patterns
Sources
Jinan

ABSTRACT

To better understand secondary aerosol pollution and potential source regions, semi-continuous measurement of water-soluble ions in $PM_{2.5}$ was performed from December 2007 to October 2008 in Jinan, the capital of Shandong Province. The data was analyzed with the aid of backward trajectory cluster analysis in conjunction with redistributed concentration field (RCF) model and principal component analysis (PCA). SO_4^{2-}, NO_3^- and NH_4^+ were the most abundant ionic species with annual mean concentrations (±standard deviations) of 38.33 (±26.20), 15.77 (±12.06) and 21.26 (±16.28) μg m^{-3}, respectively, which are among the highest levels reported in the literatures in the world. Well-defined seasonal and diurnal patterns of SO_4^{2-}, NO_3^- and NH_4^+ were observed. The fine sulfate and nitrate oxidation ratios (SOR and NOR) were much higher in summer (SOR: 0.47 ± 0.13; NOR: 0.28 ± 0.03) than those in other seasons (SOR: 0.17–0.30; NOR: 0.12–0.14), indicating more extensive formations of SO_4^{2-} and NO_3^- in summer. The most frequent air masses connected with high concentrations of SO_4^{2-}, NO_3^- and NH_4^+ originated from Shandong Province in spring, autumn and winter, while from the Yellow Sea in summer, and then slowly traveled in Shandong Province to Jinan. RCF model indicated that Shandong Province was the main potential source region for SO_4^{2-} and NO_3^- and other potential source regions were also identified including the provinces of Hebei, Henan, Anhui and Jiangsu and the Yellow Sea. Principal component analysis indicated that the major sources contributing to $PM_{2.5}$ pollution were secondary aerosols, coal/biomass burnings and traffic emissions.

1. Introduction

The rapid industrialization and urbanization in China have inevitably led to remarkable increase of air pollutants emissions in the past two decades. Coal combustions and automobile exhausts are mainly responsible for the severe air pollution in large cities in China (Chen et al., 2004). Primary air pollutants such as SO_2 and dust have been successfully reduced due to the enforcement of control measurements in recent years (Chan and Yao, 2008), while $PM_{2.5}$ has emerged as the biggest concern. $PM_{2.5}$ is believed to be a predominant factor to scatter and absorb solar radiation and reduce visibility (Sloane et al., 1991), and it can easily penetrate into lungs and lead to the respiratory and mutagenic diseases (Hughes et al., 1998). Water-soluble ions account for about half of the $PM_{2.5}$ mass (Zhang et al., 2007b; Chan and Yao, 2008). The major water-soluble ions such as sulfate, nitrate and ammonium have effects on the hydroscopic nature and acidity of aerosols (Ocskay et al., 2006), while their characteristics vary significantly with seasons and geographic locations.

Shandong Province is located on the central coast of China and adjacent to Korea and Japan. The area of Shandong constitutes only 1.6% of total China area while anthropogenic emissions from Shandong contributed approximately 10% for SO_2, 8% for NO_x, and 9% for $PM_{2.5}$ to China emissions in 2006 (National Bureau of Statistics of China, 2009; Zhang et al., 2009). Regional transport of air pollutants from Shandong was found to contribute to the aerosol pollution in Beijing under prevailing south and southeast winds (Streets et al., 2007). Besides, Shandong was identified as a potential source region for secondary inorganic aerosol in Seoul, Korea (Heo et al., 2009). As the capital of Shandong Province, Jinan was listed in the group of large cities with the highest concentrations of SO_2, NO_x and TSP in the world (Baldasano et al., 2003). Previous study showed that Jinan suffered serious $PM_{2.5}$ pollution

* Corresponding author. Environment Research Institute, Shandong University, Jinan 250100, China. Tel./fax: +86 531 88366072.
E-mail address: yanglingxiao@sdu.edu.cn (L. Yang).

1352-2310/$ – see front matter Crown Copyright © 2011 Published by Elsevier Ltd. All rights reserved.
doi:10.1016/j.atmosenv.2011.07.041

and SO_4^{2-} and NO_3^- were major contributors to the visibility reduction (Yang et al., 2007). However, temporal variations (especially diurnal variation) and source apportionments of water-soluble ions in $PM_{2.5}$ in Jinan are still unclear.

In order to better understand secondary aerosol pollution and potential source regions in Jinan, semi-continuous measurement of water-soluble ions in $PM_{2.5}$ was performed, in conjunction with trace gases and meteorological parameters in 2008. This paper presents the overall results of water-soluble ions. We first show the seasonal and diurnal variations of major water-soluble ions, and then deploy backward trajectory cluster analysis and redistributed concentration field (RCF) model to allocate the potential source regions for secondary ions in Jinan. Finally, principal component analysis (PCA) is used to uncover the underlying factors contributing to the $PM_{2.5}$ pollution in Jinan.

2. Experiments and methodologies

2.1. Sampling sites

Four intensive measurements were conducted from December 2007 to October 2008. In winter (Dec 1 2007–Jan 3 2008) and spring (Apr 1–18 2008), the observation site was chosen at the rooftop of public teaching building in Hongjialou Campus of Shandong University (in brief "HJLC"; 36°69′N, 117°06′E), and the detailed information about this site was given by Xu et al. (2010). In summer (Jun 5–17 2008) and autumn (Sep 12–Oct 15 2008), the study site was set up on the fourth floor at the building of Environmental Science and Engineering in Central Campus of Shandong University (in brief "CC"; 36°40′N, 117°03′E) (Shou et al., 2010), 1 km away from the HJLC. The sampling inlet was ~15 m above the ground level at the two sites. These two sites are both located in the urban area in Jinan, being surrounded by residential or commercial districts (Xu et al., 2010).

2.2. Instruments

An ambient ion monitor (AIM; Model URG 9000B, URG Corporation) was used to measure hourly concentrations of water-soluble ions in $PM_{2.5}$, including F^-, Cl^-, NO_2^-, NO_3^-, SO_4^{2-}, Na^+, NH_4^+, K^+, Mg^{2+} and Ca^{2+}. The instrument has been used in several field campaigns, and the details can refer to Zhou et al. (2010). To avoid positive interference from SO_2 to the SO_4^{2-} measurement (Wu and Wang, 2007; Zhou et al., 2010), a NaOH solution (5 mmol L^{-1}) was substituted for the original ultra-pure water as the denuder liquid to enhance the absorption of SO_2.

$PM_{2.5}$ samples were collected on Teflon membranes using a commercially available filter-based sampler (Reference Ambient Air Sampler, Model RAAS 2.5–400, Thermo Andersen) and 101 sets of samples were obtained during our observation. The collection of samples and analysis of water-soluble ions have been described elsewhere (Wu and Wang, 2007; Zhou et al., 2010). In this study, we compared the results obtained from AIM and traditional filter-based measurements in Section 3.1.1.

Other instruments for measuring SO_2 (TEI, Model 43C), NO_x (TEI Model 42i-TL), O_3 (TEI, Model 49C), CO (API Model 300E) and BC (Magee Scientific, Berkeley, California, USA, Model AE-21) have been described in our previous studies (Zhou et al., 2009; Wang et al., 2010). And the meteorological data were directly obtained from an automatic meteorological station (Xu et al., 2010).

2.3. Trajectories calculation and cluster analysis

Three-day backward trajectories, terminated at 50 m a.s.l., were computed every hour by the Hybrid Single-Particle Lagrangian Integrated Trajectory model (HYSPLIT, version 4.9) with the Global Data Assimilation system (GDAS) meteorological data (Draxler and Rolph, 2003). A total of 2278 backward trajectories with 72 hourly trajectory endpoints in four seasons were used as input for further analysis. A K-means cluster approach was then used to classify the trajectories into several different clusters (Salvador et al., 2010) and five suitable clusters were chosen in four seasons.

2.4. Redistributed concentration field (RCF) model

In this study, C_k is the concentration measured at the receptor site for trajectory k. If C_{ik} is the mean concentration of the grid cells which are hit by segment i ($i = 1, N_k$) of trajectory k (Salvador et al., 2010), then the distribution of air pollutants for trajectory k is

$$C_{ik} = C_k \frac{C_{ik} N_k}{\sum_{i=1}^{N_k} C_{ik}},\ i = 1, N_k \tag{1}$$

After the redistribution of all individual trajectories, the new concentration field $\overline{C}_{mn}$ is calculated by the redistributed concentration C_{ik}:

$$\log\overline{C}_{mn} = \frac{1}{\sum_{k=1}^{M}\sum_{i=1}^{N_k}\tau_{mnik}} \sum_{k=1}^{M}\sum_{i=1}^{N_k} \log(C_{ik})\tau_{mnik} \tag{2}$$

In eq. (2), τ_{mnil} is the residence time of segment i for trajectory k in grid cell (m, n). The new concentration filed is repeated until the average difference for the concentration fields of two successive iterations is below a threshold value of 0.5%. The geophysical regions passed by the trajectories were divided into 1.0° × 1.0° grids.

3. Results and discussions

3.1. Overall statistics of water-soluble ions in $PM_{2.5}$

3.1.1. Comparison of results from AIM and traditional filter-based measurements

To evaluate the performance of modified AIM, hourly data from AIM were averaged to match the collection time of filter samples for comparison. The results from AIM and traditional filter-based measurements are plotted in Fig. 1. Excellent correlations were found for major ionic species, namely, SO_4^{2-}, NO_3^-, NH_4^+, Cl^- and K^+ (R^2 = 0.84–0.95, RMA slope = 0.83–1.08), and good correlations (R^2 = 0.46–0.90, RMA slope = 0.83–1.08) were obtained for F^-, Na^+, Mg^{2+} and Ca^{2+} with relatively low concentrations. NO_2^- showed no correlation and far higher concentration measured by AIM than that by traditional filter-based measurement (RMA slope = 42.90; R^2 = 0.08), and this difference could be due to the loss of NO_2^- from the filters (Chang et al., 2007; Zhang et al., 2007a). Overall, AIM worked well for measuring major water-soluble ions in $PM_{2.5}$.

3.1.2. Mass concentrations

The hourly mean concentrations and standard deviations of water-soluble ions in $PM_{2.5}$ are summarized in Table 1. The concentrations of water-soluble ions followed the order of $SO_4^{2-} > NH_4^+ > NO_3^- > Cl^- \sim NO_2^- \sim K^+ > Na^+ > Ca^{2+} > F^- > Mg^{2+}$ and this order changed slightly with seasons. SO_4^{2-}, NH_4^+ and NO_3^- were the dominant ions, and contributed more than 80% to the total measured water-soluble ions. SO_4^{2-} was the most abundant water-soluble ion in Jinan and its annual mean concentration was 38.33 ± 26.20 μg m^{-3}, accounting for 44.65 ± 11.30% of the total measured water-soluble ions. It is worth noting that the concentration of SO_4^{2-} alone was more than twice the annual US National

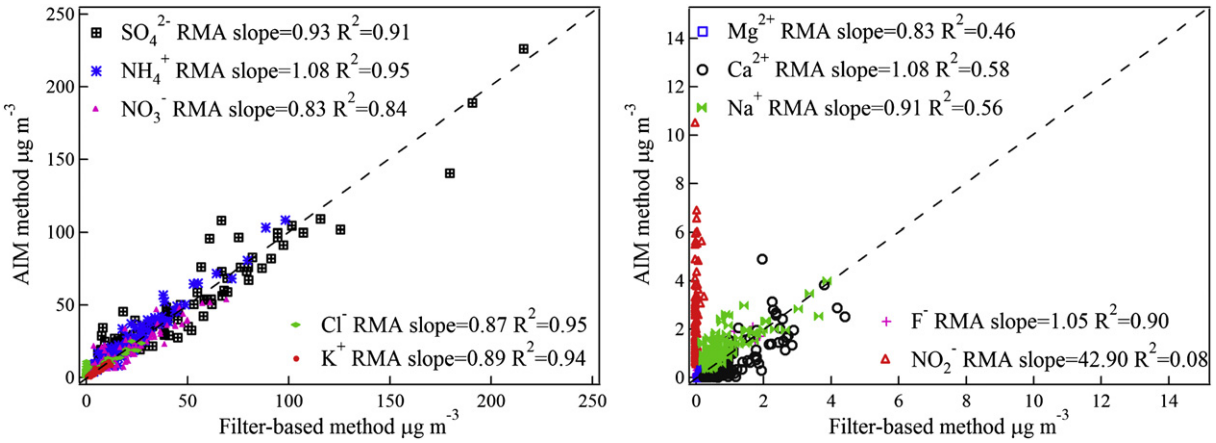

Fig. 1. Scatter plots of major water-soluble ions from AIM and Filter-based methods.

Ambient Air Quality Standards of $PM_{2.5}$ (15 μg m^{-3}) and the hourly maximum concentration of SO_4^{2-} could be up to 227 μg m^{-3}. NH_4^+ (21.16 ± 16.28 μg m^{-3}) and NO_3^- (15.77 ± 12.06 μg m^{-3}) were another major components, accounting for 17.63 ± 7.61% and 23.07 ± 5.85% of the total water-soluble ions respectively.

Table 2 compares the concentrations of SO_4^{2-}, NH_4^+ and NO_3^- in $PM_{2.5}$ in Jinan with those measured in other cities over the world. Obviously, the levels of these compounds in Jinan were substantially (5–10 times) higher than those in cities of USA, Europe, Japan and Korea. Moreover, they were also higher than those of other Chinese cities (e.g. Beijing, Shanghai), which are well-known to suffer serious aerosol pollution. These results demonstrated the severity of secondary inorganic aerosol pollution in Jinan.

3.2. Temporal variations of water-soluble ions in $PM_{2.5}$

3.2.1. Seasonal variations of major water-soluble ions

Different seasonal variations were observed for individual ion due to their differences in emission sources and formation mechanisms (Table 1). Secondary ions, namely SO_4^{2-}, NO_3^-, NH_4^+ and NO_2^- showed higher values in summer (64.27 ± 31.00, 19.22 ± 11.84, 28.01 ± 16.27 and 2.93 ± 2.45 μg m^{-3}) and winter (42.84 ± 31.72, 21.77 ± 15.05, 29.19 ± 20.72 and 2.48 ± 1.94 μg m^{-3}), and lower levels in spring (27.11 ± 11.41, 10.19 ± 6.00, 13.28 ± 8.75 and 1.50 ± 1.27 μg m^{-3}) and autumn (30.99 ± 14.15, 11.69 ± 7.33, 15.13 ± 7.36 and 1.75 ± 1.61 μg m^{-3}). The summertime peak could be attributed to more active photochemistry process which can facilitate formation of secondary species, while the higher levels in winter may associate with huge emissions of primary pollutants (such as SO_2 and NO_x) from coal combustion for heating and worsen atmospheric dispersion.

The fine sulfate and nitrate oxidation ratios (SOR and NOR) are defined as $SOR = nSO_4^{2-}/(nSO_4^{2-} + nSO_2)$ and $NOR = nNO_3^-/(nNO_3^- + nNO_x)$ to indicate the process and extent of formations from SO_2 to SO_4^{2-} and NO_x to NO_3^- (Wang et al., 2005). SOR and NOR are represented in Fig. 2 and their average values were both larger than 0.10, reflecting occurrence of secondary formation in Jinan (Wang et al., 2005). SOR in summer was 0.47 ± 0.13, much larger than that in spring (0.22 ± 0.05), autumn (0.30 ± 0.04) and winter (0.17 ± 0.02), indicating stronger oxidation of SO_2 to SO_4^{2-} in summer leading to the highest concentration of SO_4^{2-} in spite of relatively lower SO_2 concentrations among four seasons (SO_2: Summer = 26.25 ± 28.73 ppb; Spring = 32.14 ± 26.86 ppb; Autumn = 22.31 ± 16.41 ppb; Winter = 58.59 ± 32.98 ppb). The formation of SO_4^{2-} from SO_2 mainly includes gas-phase reaction of SO_2 and OH radical affected by temperature and solar radiation (Seinfeld, 1986), and heterogeneous reaction which is a function of RH (metal catalyzed oxidation or H_2O_2/O_3 oxidation) (Dlugi et al., 1981). The seasonal variation of SOR was consistent with temperature in Fig. 2, indicating that gas-phase oxidation of SO_2 played a major role in the formation of SO_4^{2-} in the whole year (Wang et al., 2005). NOR showed the highest level in summer (0.28 ± 0.03), the lowest level in winter (0.12 ± 0.01), and comparable level in spring (0.14 ± 0.01) and autumn (0.14 ± 0.01), indicating that high temperature and high RH promoted the faster formation of NO_3^- in spite of more dissociation of NH_4NO_3 at high temperature in summer.

The mass ratio of NO_3^-/SO_4^{2-} has been used as an indicator of relative importance of mobile (e.g. vehicles) vs. stationary sources (e.g. power plant) in the air pollution (Yao et al., 2002; Wang et al., 2006). High NO_3^-/SO_4^{2-} mass ratios have been measured in southern California, with 2 in downtown Los Angeles and 5 in

Table 1
Concentrations of water-soluble ions (mean concentrations ± standard deviation (SD)) in four seasons in Jinan (μg m^{-3}).

Species	Mean ± SD				
	Annual (N = 2282)	Spring (N = 448)	Summer (N = 276)	Autumn (N = 773)	Winter (N = 785)
F^-	0.33 ± 0.42	0.22 ± 0.31	0.21 ± 0.28	0.15 ± 0.15	0.61 ± 0.53
Cl^-	4.19 ± 5.36	1.59 ± 2.34	3.18 ± 3.74	1.44 ± 1.56	8.75 ± 6.37
NO_2^-	2.10 ± 0.86	1.50 ± 1.27	2.93 ± 2.45	1.75 ± 1.61	2.48 ± 1.94
NO_3^-	15.77 ± 12.06	10.19 ± 6.00	19.22 ± 11.84	11.69 ± 7.33	21.77 ± 15.05
SO_4^{2-}	38.33 ± 26.20	27.11 ± 11.41	64.27 ± 31.00	30.99 ± 14.15	42.84 ± 31.72
Na^+	1.22 ± 0.75	0.85 ± 0.38	2.12 ± 1.04	1.04 ± 0.62	1.34 ± 0.65
NH_4^+	21.26 ± 16.28	13.28 ± 8.75	28.01 ± 16.27	15.13 ± 7.361	29.19 ± 20.72
K^+	2.36 ± 2.32	1.32 ± 1.14	4.62 ± 3.08	1.44 ± 1.17	3.07 ± 2.54
Mg^{2+}	0.11 ± 0.15	0.12 ± 0.10	0.03 ± 0.05	0.01 ± 0.07	0.22 ± 0.17
Ca^{2+}	0.76 ± 1.18	0.83 ± 0.17	0.29 ± 0.46	0.23 ± 0.59	1.41 ± 1.43

Table 2
Mass concentrations of $PM_{2.5}$ and the major chemical components in Jinan and other cities over the world (μg m^{-3}).

Site	Type	Time	Mass concentrations (μg m^{-3})				References
			$PM_{2.5}$	SO_4^{2-}	NH_4^+	NO_3^-	
Jinan, China	Urban	Dec 2007–Oct 2008		38.33	21.26	15.77	This study
Beijing, China	Urban	2001–2003	154.26	17.07	8.72	11.52	Wang et al., 2005
Shanghai, China	Urban	Sep 2003–Jan 2005	94.64	10.39	3.78	6.23	Wang et al., 2006
Qingdao, China	Coastal	1997–2000	43.6	11.94	5.79	3.4	Hu et al., 2002
Xi'an, China	Urban	Oct 2006–Sep 2007	130	27.9	7.6	12	Shen et al., 2009
Linan, China	Rural	Oct–Nov 1999	90	21.2	8.6	7.7	Xu et al., 2002
Mong Kok, Hong Kong	Urban	Nov 2000–Feb 2001	69.15	10.32	3.84	2.65	Louie et al., 2005
Taichung, Taiwan	Urban	2001–2003	59.8	9.45	4.49	1.93	Fang et al., 2002
Seoul, Korea	Urban	Mar 2003–Feb 2005	42.8	7.5	5.5	7.1	Kim et al., 2007
Tokyo, Japan	Urban	Sep 2007–Aug 2008	20.58	3.8	2.27	0.96	Khan et al., 2010
New York, US	Urban	2002–2003	13.16	4.29	1.93	2.04	Qin et al., 2006
St. Louis, US	Urban	2000–2003	16.4	4.23	1.94	2.48	Lee and Hopke, 2006
Kerbside, Switzerland	Urban	Apr 1998–Mar 1999	24.6	2.8	1.6	3	Hueglin et al., 2005
Huelva, Spain	Urban	1999–2005	19	3.6	1.4	0.5	Querol et al., 2008
Milan, Italy	Urban	Aug 2002–Nov 2003	20.2	4	2.2	4.6	Lonati et al., 2005
Milan, Italy	Urban	Aug 2002–Nov 2003	53.7	5.8	5.2	20.2	Lonati et al., 2005

Rubidoux, which was due to less use of coal (Kim et al., 2000); However in Chinese cities (e.g. Beijing, Shanghai), lower ratios had been reported as a result of the wide use of sulfur-containing coal (Yao et al., 2002). In our study, the NO_3^-/SO_4^{2-} mass ratio ranged from 0.03 to 1.52, with the annual mean of 0.44. These results indicated that like other cities in China, stationary sources were more important compared with vehicle emissions in Jinan. The NO_3^-/SO_4^{2-} mass ratios showed clear seasonal variations with the highest ratio in winter (0.53 ± 0.05), the lowest ratio in summer (0.34 ± 0.03), and comparable ratio in spring (0.40 ± 0.06) and autumn (0.42 ± 0.06) (see Fig. 2). The reason is that in summer high temperature and high RH are more favorable for formation of SO_4^{2-} compared to NO_3^- due to enhanced evaporation of NH_4NO_3 at high temperature.

Cl^- showed higher concentrations in winter (8.75 ± 6.37 μg m^{-3}) than that in other seasons (Table 1). Cl^- is a major component of sea-salt particle, and is also released from coal combustion (Sun et al., 2006). In winter, the air generally originated from the northwest (Xu et al., 2010) and thus the influence of sea-salt would be minor. The mass ratio of Cl^-/Na^+ was calculated as 6.18 ± 2.96 in winter, which is much higher than that detected for sea water (1.797) (Moller, 1990). Therefore, the elevated concentration of Cl^- in winter was due to the enhanced coal combustion. K^+ exhibited higher levels in summer (4.62 ± 3.08 μg m^{-3}) and winter (3.07 ± 2.54 μg m^{-3}) than that in spring and autumn (1.32 ± 1.14 and 1.44 ± 1.17 μg m^{-3}). In summer, extensive activities of biomass burning around Shandong was the main factor contributing to the elevated concentration of K^+ (http://maps.geog.

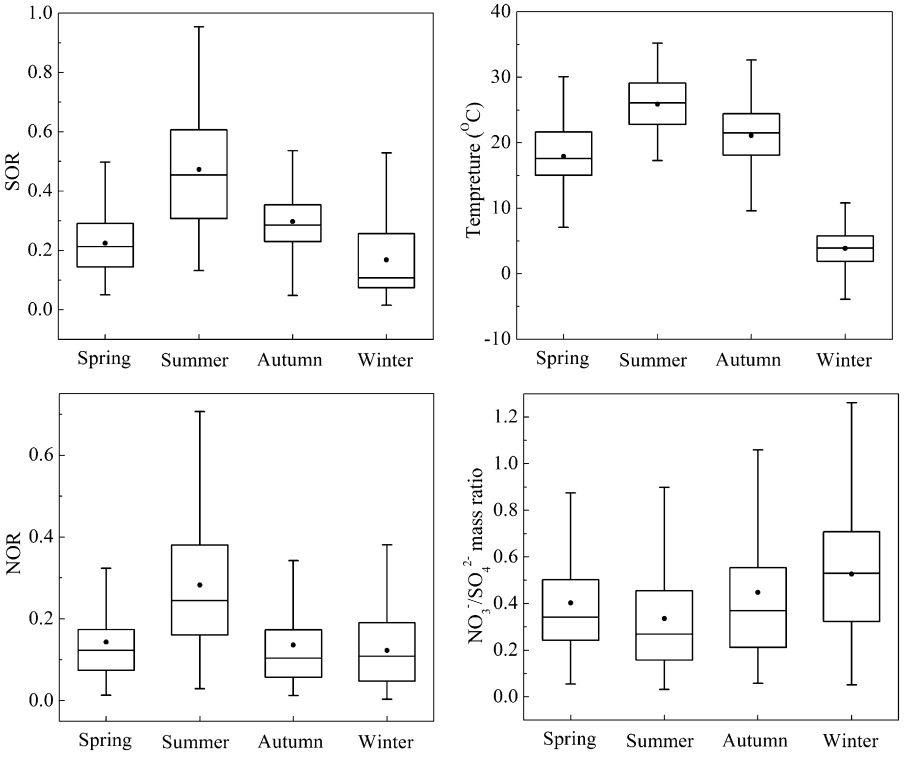

Fig. 2. Seasonal variations of SOR, NOR, NO_3^-/SO_4^{2-} mass ratio and temperature.

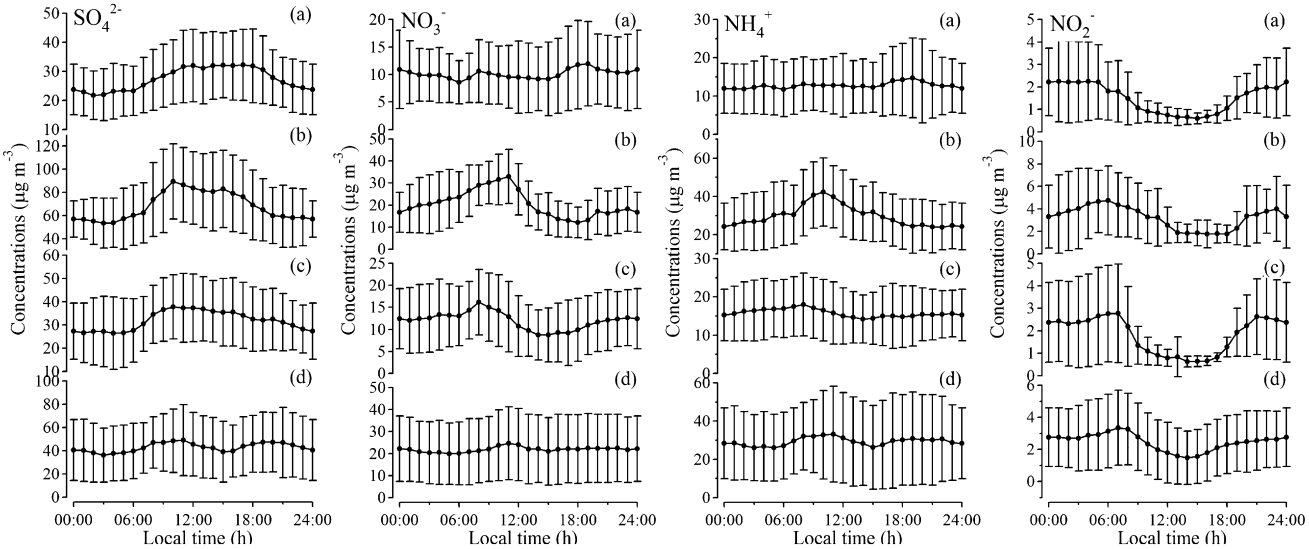

Fig. 3. The diurnal profiles of SO_4^{2-}, NO_3^-, NH_4^+ and NO_2^- in four seasons (a) Spring; (b) Summer; (c) Autumn; (d) Winter.

umd.edu/firms/). High concentrations of K^+ in winter may be associated with coal combustion as implied from the strong correlation ($r = 0.82$) between K^+ with Cl^- (Westberg et al., 2003). Other water-soluble ions were not relevant for seasonal variations due to their low concentrations.

3.2.2. Diurnal variations of secondary water-soluble ions

The diurnal variations of secondary water-soluble ions in $PM_{2.5}$ in four seasons are shown in Fig. 3. In general, SO_4^{2-} exhibited similar diurnal profiles in spring, summer and autumn, with an evident increase as sun rising and a broad daytime maximum, which was consistent with those reported in other cities (e.g. Beijing, PRD) (Hu et al., 2008; Wu et al., 2009). This typical pattern can be explained by the fact that photochemical production is more extensive during the daytime with stronger solar radiation. Compared with other seasons, in winter SO_4^{2-} had a little diurnal variation and showed two peaks in the morning and evening, which may be related with boundary layer height and photochemical

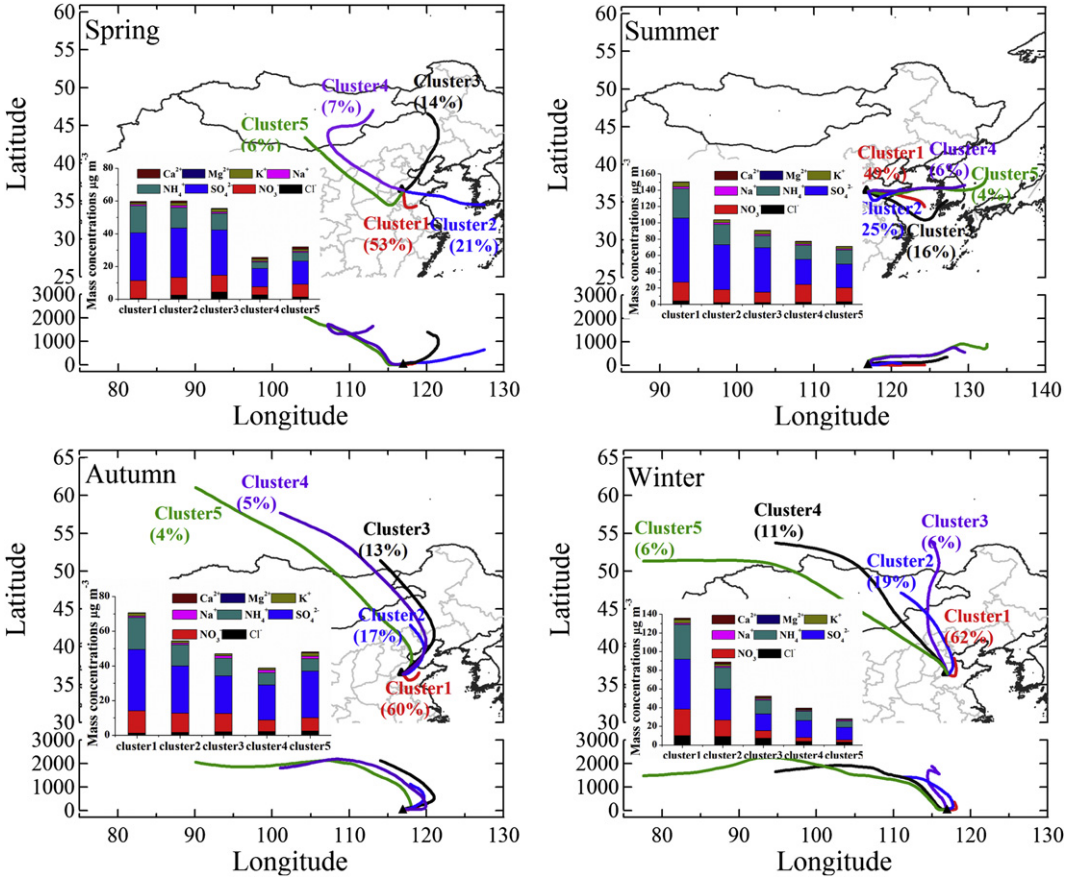

Fig. 4. Mean clusters and the corresponding mean ions concentrations in four seasons.

reaction. The morning peak may be contributed to enhanced photochemical production and the evening peak was a result of accumulation of pollutants with reduced boundary layer height. The lower concentration in the early afternoon was because that the dilution of SO_4^{2-} by increase of boundary layer overwhelmed the production of SO_4^{2-} caused by photochemical reactions.

NO_3^- had a more apparent diurnal profile in summer and autumn than that in spring and winter. In summer and autumn, NO_3^- peaked in the morning, and its lowest concentration appeared at 16:00–18:00 (Hu et al., 2008; Wu et al., 2009). The morning peak was synchronous with NO_x, indicating its relation to vehicle emissions (Park et al., 2005). The lowest concentration of NO_3^- in the afternoon was attributed to dissociation of NH_4NO_3 at high temperature and increase of boundary layer height. In winter and spring NO_3^- showed a little diurnal pattern, which was due to minor influence of thermodynamic equilibrium at low temperature. NO_3^- showed two peaks in the morning and evening in spring which was consistent with that of NO_x and may be associated with vehicle emissions (Park et al., 2005). In four seasons NH_4^+ showed similar diurnal profiles with SO_4^{2-} or NO_3^-, indicating the existences of $(NH_4)_2SO_4$ and NH_4NO_3.

NO_2^- showed similar diurnal profiles in four seasons with higher concentrations at night and lower concentrations during daytime (Fig. 3), and similar profile was also observed in Beijing (Zhang et al., 2007a). Higher NO_2^- concentration at night than that during daytime probably was related with lower oxidized extent due to weak solar radiation and nighttime accumulation of NO_2^-.

3.3. Sources

3.3.1. The potential source regions identification using trajectory statistical methods

Backward trajectory cluster analysis is a useful tool to evaluate the origins of air pollutants at the receptor sites (Salvador et al., 2010), and redistributed concentration field (RCF) model can estimate the potential source regions (Stohl, 1996). The combination of backward trajectory cluster analysis and RCF model can be better to provide a comprehensive view of the potential source regions for SO_4^{2-} and NO_3^- in $PM_{2.5}$ in Jinan. Three-day mean trajectories for clusters in spring, summer, autumn and winter and corresponding mean concentrations of water-soluble ions are expressed in Fig. 4. All the trajectories in four seasons can be classified into 4 main categories based on their origins, paths and latitudes: (1) the shortest/local transport pattern, (2) eastern airflow, (3) northeast air masses and (4) northwest/north air parcel with long transport path. From Fig. 4, it can be seen that the shortest/local transport pattern (cluster 1) was frequent and accounted for 53% of total trajectories in spring, 49% in summer, 60% in autumn and 62% in winter. Eastern airflow was dominant in summer and contributed for 21% of total trajectories in spring (cluster 2). Northeast/north air masses were observed in spring (cluster 3, 14%) and in autumn (cluster 2, 17%). Other clusters generally originated from northwest/north of China and traveled fast at the highest altitude.

The highest concentrations of SO_4^{2-}, NO_3^- and NH_4^+ were observed in the shortest cluster (cluster 1) in four seasons, indicating that secondary ions in $PM_{2.5}$ were easy to be enriched in the

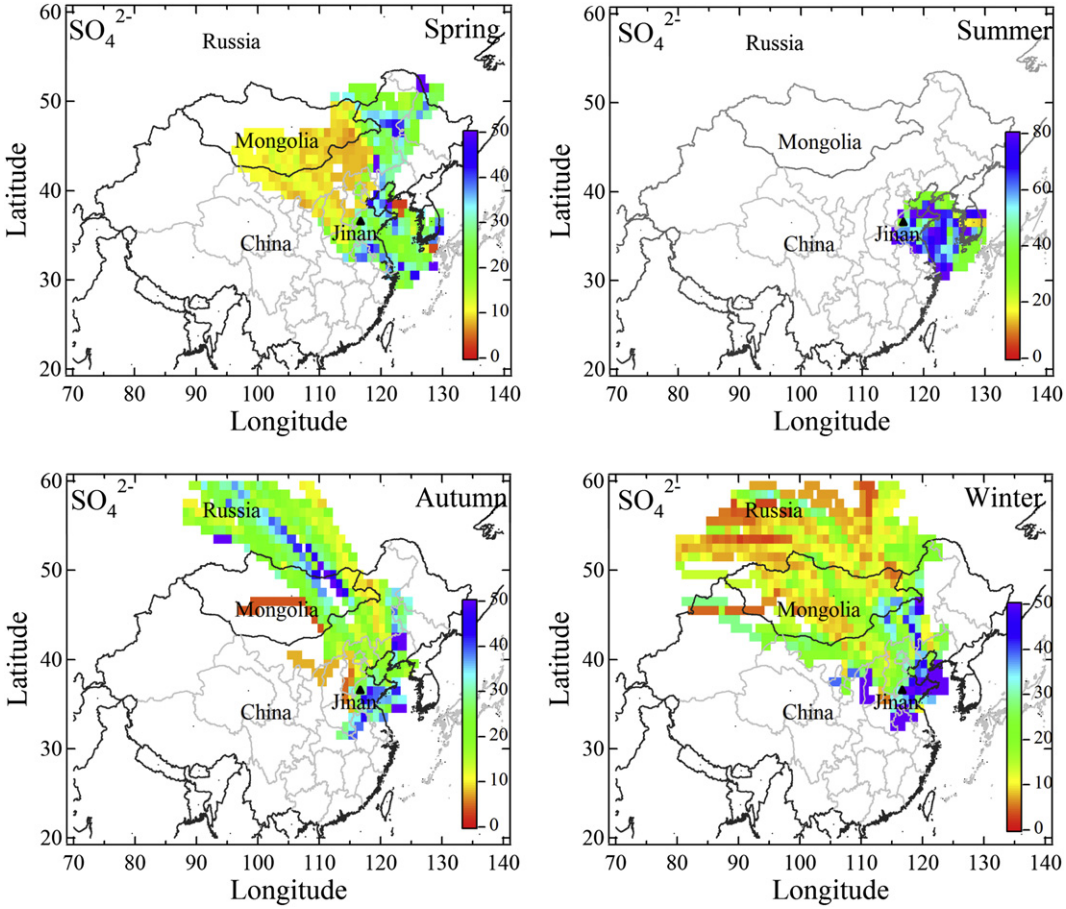

Fig. 5. RCF distribution for sulfate in Jinan in four seasons.

short trajectories from upwind regional and local emission sources (Karaca and Camci, 2010). Cluster 1 generally originated from the middle of Shandong Province, moved southerly and finally turned westerly to Jinan in spring, autumn and winter, while in summer it derived from the Yellow Sea, moved northwesterly to Jinan. A major big petro-chemical corporation, power plants and cement production base are located in the middle (Zibo city) and southwest (Jining city and Zaozhuang city) of Shandong Province. Cluster 1 spent much time on passing over industrial zones with high emissions of primary pollutants (e.g. SO_2, NO_x), leading to the high concentrations of SO_4^{2-}, NO_3^- and NH_4^+.

Much higher concentrations of SO_4^{2-}, NO_3^- and NH_4^+ were associated with air masses from northeast or northwest, including cluster 3 in spring, clusters 2 in autumn and cluster 2 in winter. The flow patterns of cluster 3 in spring and cluster 2 in autumn were both typically originated from Inner Mongolia, flowed over Liaoning Province and Bohai Gulf before arriving at Jinan. While cluster 2 in winter derived from Outer Mongolia, passed through Inner Mongolia, Hebei Province and then to Jinan. These trajectories all passed over the Bohai economic zone, which is one of the most populated and industrial zones in China and has the highest SO_2 and NO_x emissions (Zhang et al., 2009).

Low concentrations of SO_4^{2-}, NO_3^- and NH_4^+ occurred in cluster 4 and 5 in spring, autumn and winter. These clusters derived from northwest of China and moved faster at the higher latitudes compared to other clusters.

Compared to other seasons, in summer higher concentrations of SO_4^{2-}, NO_3^- and NH_4^+ could be explained by the combination of Dimethyl Sulfide (DMS) oxidation (Salvador et al., 2010) and long residence time over industrial zones with large amount emissions of primary pollutants. It was worth noting that there was also a significant fraction of the flow from Korea in summer (cluster 4 and 5, 10%), which passed westerly over the Yellow Sea and Jiaodong Peninsula before arriving at Jinan.

Figs. 5 and 6 show the results of RCF analysis for SO_4^{2-} and NO_3^-, respectively. The high potential source region of SO_4^{2-} and NO_3^- was Shandong, and Hebei, Henan, Anhui, Jiangsu, Liaoning, and Inner Mongolia in spring, autumn and winter and eastern Jiangsu Province, South Korea and the Yellow Sea in summer were also identified as the potential source regions.

3.3.2. *The sources identification by principal component analysis (PCA)*

In order to identify the sources of water-soluble ions in $PM_{2.5}$, principal component analysis (PCA) was applied. PCA is a widely used statistical technique to quantitatively identify a smaller number of independent factors among the compound concentrations, which can explain the variance of the data, by using the eigenvector decomposition of a matrix of pair-wise correlations (Johnson and Wichern, 1998; Miller et al., 2002). PCA is conducted using a commercially available software package (SPSS). Hourly values of Nss-SO_4^{2-}, NO_3^-, NH_4^+, Cl^-, NO_2^-, Na^+, K^+, Mg^{2+}, Ca^{2+}, NO_x, SO_2, CO, BC and O_3 were used for PCA and the results are shown in Table 3.

In spring, four principal components were obtained and accounted for 82% of the total variance. The principal component 1 accounted for 45% of the total variance, and comprised NO_x, NO_2^-, BC and CO, while anti-correlated with O_3, indicating its relation to

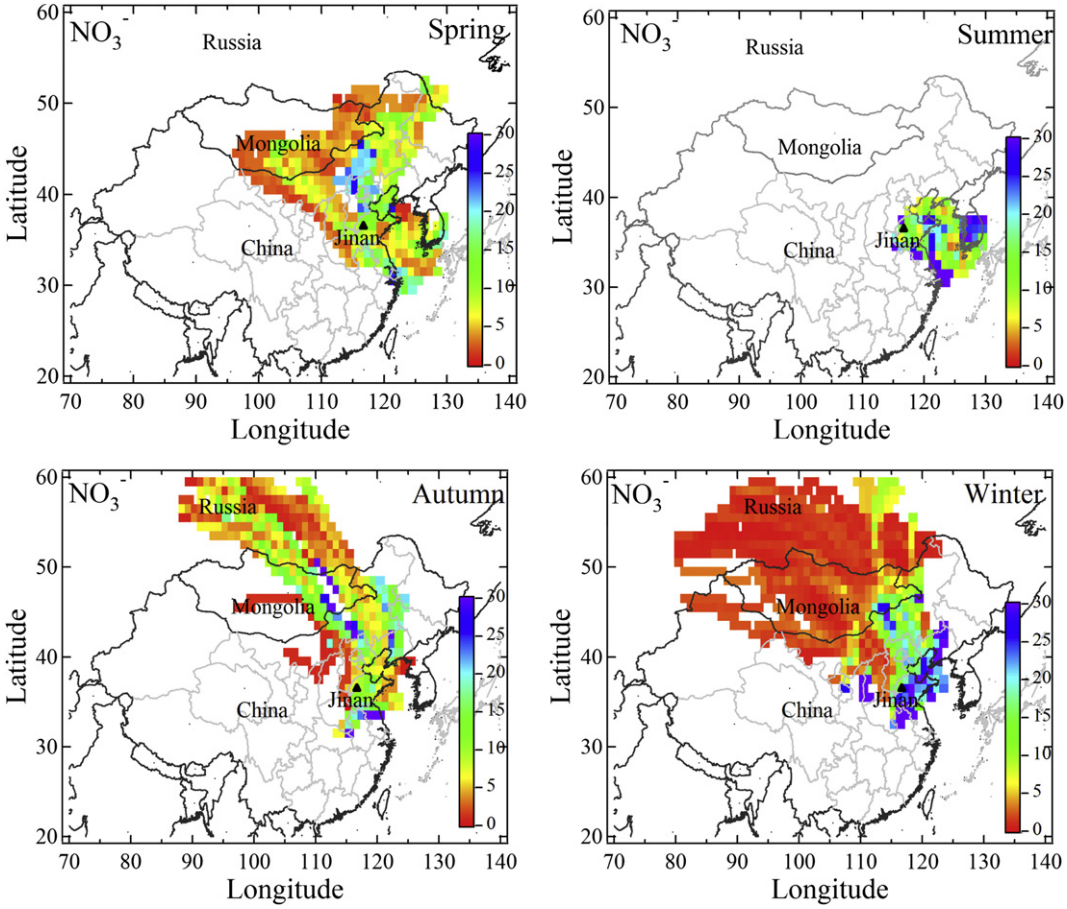

Fig. 6. RCF distribution for nitrate in Jinan in four seasons.

Table 3
Factor loadings from PCA in the four seasons.

	Spring				Summer			Autumn			Winter		
	1	2	3	4	1	2	3	1	2	3	1	2	3
Nss-SO_4^{2-}	−0.08	**0.76**	**0.51**	0.11	**0.73**	−0.06	0.56	**0.94**	0.03	0.04	**0.93**	−0.11	0.10
NO_3^-	0.20	**0.91**	0.02	0.03	**0.91**	0.18	−0.07	**0.63**	0.49	−0.24	**0.78**	−0.18	0.26
NH_4^+	0.21	**0.84**	0.28	0.14	**0.90**	0.05	0.35	**0.91**	0.44	−0.19	**0.95**	−0.03	0.12
Cl^-	0.46	−0.08	**0.78**	−0.12	**0.75**	0.41	−0.07	0.40	0.03	0.23	**0.85**	0.40	0.05
NO_2^-	**0.85**	0.27	0.17	0.09	0.38	**0.76**	−0.01	−0.05	**0.77**	0.06	**0.83**	0.15	−0.03
Na^+	0.01	0.27	0.68	0.48	0.12	0.23	0.45	−0.01	0.04	**0.67**	**0.84**	0.15	−0.01
K^+	0.39	0.26	0.55	0.32	**0.87**	−0.02	0.09	**0.69**	0.20	0.50	**0.91**	0.06	0.06
Mg^{2+}	0.12	0.17	0.05	**0.95**	0.30	**0.61**	0.02	0.08	0.17	**0.72**	0.28	**0.74**	0.14
Ca^{2+}	0.23	−0.02	−0.03	**0.89**	−0.10	**0.84**	0.02	0.05	0.45	**0.78**	0.20	**0.86**	−0.11
NOx	**0.83**	0.13	0.22	0.30	0.18	**0.84**	0.23	0.00	**0.73**	0.53	−0.19	0.36	**0.69**
SO_2	0.11	0.25	**0.77**	−0.18	−0.02	−0.11	**0.85**	**0.69**	−0.22	0.37	−0.14	**0.74**	0.25
CO	**0.57**	0.31	**0.57**	0.22	**0.71**	0.60	0.21	0.31	0.73	0.34	**0.81**	0.41	−0.08
O_3	**−0.88**	0.09	−0.17	−0.01	−0.23	**−0.75**	0.36	0.26	**−0.42**	−0.07	−0.32	0.03	**−0.64**
BC	**0.70**	−0.08	0.00	0.42	**0.72**	0.41	−0.10	0.29	**0.83**	0.25	**0.85**	0.33	−0.05
Variance	45%	15%	13%	9%	45%	18%	10%	39%	18%	12%	52%	16%	7%

Note: Values in bold indicate loading factors discussed in this paper.

traffic emissions. The principal component 2 could be explained by secondary aerosols due to the positive contribution from Nss-SO_4^{2-}, NO_3^- and NH_4^+, and this factor accounted for 15% of the total variance. The principal component 3 contained Cl^- and SO_2 with 13% of the total variance, which was related with stationary source emissions such as coal combustion. The principal component 4 was primarily composed of Ca^{2+}, Mg^{2+} and Na^+, and was attributed to the crustal and soil dust from urban constructions.

In summer, three principal components were identified and accounted for 73% of the total variance. The principal component 1 had highly positive contributions from Nss-SO_4^{2-}, NO_3^-, NH_4^+, Cl^-, K^+, BC and CO, which could be explained by secondary aerosols mixing with biomass burning. In summer, extensive activities of biomass burning around Shandong were observed (http://maps.geog.umd.edu/firms/) and biomass burning is likely to emit large amount of Cl^-, K^+, BC and CO. The principal component 2 was composed of NO_x, NO_2^-, Ca^{2+} and Mg^{2+}, and anti-correlated with O_3, which was identified as traffic emissions mixing with crustal and soil dust. The principal component 3 was composed of SO_2, mainly from coal combustion.

In autumn, three principal components were identified and accounted for 69% of the total variance. The principal component 1 accounted for 39% of the total variance, which could be explained by secondary aerosols due to the positive contribution from Nss-SO_4^{2-} NO_3^- and NH_4^+. The principal component 2 was composed of NO_x, NO_2^-, CO and BC, and anti-correlated with O_3, indicating its relation to traffic emissions which accounted for 18% of the total variance. The principal component 3 was primarily composed of Ca^{2+}, Mg^{2+} and Na^+, and was attributed to the crustal and soil dust from urban constructions.

In winter, three principal components also were obtained. The principal component 1 could be identified as secondary aerosols mixing with coal combustion due to the positive combustion from Nss-SO_4^{2-}, NO_3^-, NH_4^+, Cl^-, NO_2^-, Na^+, K^+, BC and CO. The principal components 2 and 3 were composed of primary pollutants (e.g. SO_2, NO_x, Ca^{2+}, Mg^{2+}), mainly from coal combustion, crustal and soil dust and traffic emissions. These components accounted for 75% of the total variance in winter.

All in all, the source apportionment indicated that secondary aerosols, coal/biomass burnings and traffic emissions were major contributors for $PM_{2.5}$ loading in Jinan.

4. Summary

Hourly concentrations of water-soluble ions in $PM_{2.5}$ were measured to investigate secondary aerosol pollution and potential source regions in Jinan, Shandong Province from Dec 2007 to Oct 2008.

The results verified that Jinan was suffering more serious fine particle pollution compared with other cities in the world. Accelerated photochemistry reaction under high temperature, O_3 concentrations and strong solar radiation in summer and high emissions of SO_2 and NO_x from coal combustion in winter led to higher concentrations of SO_4^{2-}, NO_3^- and NH_4^+ in these two seasons than those in spring and autumn. The diurnal variations of SO_4^{2-} in spring, autumn and winter were dominated by photochemical process, while in winter controlled by boundary layer height and photochemical reaction. In summer and autumn thermodynamic reaction affected diurnal variation of NO_3^-, while it rarely occurred in spring and winter with a little diurnal variation. Production of secondary inorganic aerosol was more extensive in summer implied by higher SOR and NOR compared to other seasons.

Cluster analysis showed that the synoptic flows arriving at Jinan were dominated by the air masses originating and circulating locally in Shandong Province in spring, autumn and winter, while originating from the Yellow Sea in summer. RCF results indicated that the major potential source regions for secondary ions were concentrated in Shandong and partly from the provinces of Hebei, Henan, Anhui, Jiangsu, and Liaoning, as well as Inner Mongolia in spring, autumn and winter, while in summer Shandong, eastern Jiangsu, South Korea and the Yellow Sea were identified as the main potential source regions. Secondary aerosol dominated the variations of aerosol loading. Traffic emissions and coal combustions were major contributors for urban pollution. The influence of biomass burnings in summer was observed in Jinan.

Acknowledgments

This work was supported by the National Basic Research Program (973 Program) of China (2005CB422203), a key project of Shandong Provincial Environmental Agency (2006045), Promotive Research Fund for Young and Middle-aged Scientists of Shandong Province (BS2010HZ010) and Independent Innovation Foundation of Shandong University (2009TS024).

References

Baldasano, J.M., Valera, E., Jiménez, P., 2003. Air quality data from large cities. Science of Total Environment 307 (1–3), 141–165.
Chan, C.K., Yao, X.H., 2008. Air pollution in mega cities in China. Atmospheric Environment 42 (1), 1–42.

Chang, S.Y., Lee, C.T., Chou, C.C.K., Liu, S.C., Wen, T.X., 2007. The continuous field measurements of soluble aerosol compositions at the Taipei Aerosol Supersite, Taiwan. Atmospheric Environment 41 (9), 1936–1949.

Chen, B.H., Hong, C.J., Kan, H.D., 2004. Exposures and health outcomes from outdoor air pollutants in China. Toxicology 198 (1–3), 291–300.

Dlugi, R., Jordan, S., Lindemann, E., 1981. The heterogeneous formation of sulfate aerosols in the atmosphere. Journal of Aerosol Science 12, 185–197.

Draxler, R.R., Rolph, G.D., 2003. HYSPLIT (Hybrid Single-Particle Lagrangian Integrated Trajectory) Model Access via NOAA ARL READY Websiter. NOAA Air Resources Laboratory, Silver Spring, MD. Available at: http://www.arl.noaa.gov/HYSPLIT.php (accessed 2009).

Fang, G.C., Chang, C.N., Wu, Y.S., Fu, P.P.C., Yang, C.J., Chen, C.D., Chang, S.C., 2002. Ambient suspended particulate matters and related chemical species study in central Taiwan, Taichung during 1998–2001. Atmospheric Environment 36 (12), 1921–1928.

Heo, J.B., Hopke, P.K., Yi, S.M., 2009. Source apportionment of $PM_{2.5}$ in Seoul, Korea. Atmospheric Chemistry and Physics 9, 4957–4971.

Hu, M., Wu, Z.J., Slanina, J., Lin, P., Liu, S., Zeng, L.M., 2008. Acidic gases, ammonia and water-soluble ions in $PM_{2.5}$ at a coastal site in the Pearl River Delta, China. Atmospheric Environment 42 (25), 6310–6320.

Hueglin, C., Gehrig, R., Baltensperger, U., Gysel, M., Monn, C., Vonmont, H., 2005. Chemical characterisation of $PM_{2.5}$, PM_{10} and coarse particles at urban, near-city and rural sites in Switzerland. Atmospheric Environment 39 (4), 637–651.

Hughes, L.S., Cass, G.G., Gone, J., Ames, M., Olmez, I., 1998. Physical and chemical characterization of atmospheric ultrafine particles in the Los Angeles area. Environmental Science & Technology 32 (9), 1153–1161.

Hu, M., He, L.Y., Zhang, Y.H., Wang, M., Kim, Y.P., Moon, K.C., 2002. Seasonal variation of ionic species in fine particles at Qingdao, China. Atmospheric Environment 36 (38), 5853–5859.

Johnson, R.A., Wichern, D., 1998. Applied Multivariate Statistical Analysis. Prentice Hall, Englewood Cliffs, NJ.

Karaca, F., Camci, F., 2010. Distant source contributions to PM_{10} profile evaluated by SOM based cluster analysis of air mass trajectory sets. Atmospheric Environment 44 (7), 892–899.

Khan, M.F., Shirasuna, Y., Hirano, K., Masunaga, S., 2010. Characterization of $PM_{2.5}$, $PM_{2.5-10}$ and $PM_{>10}$ in ambient air, Yokohama, Japan. Atmospheric Research 96 (1), 159–172.

Kim, B.M., Teffera, S., Zeldin, M.D., 2000. Characterization of $PM_{2.5}$ and PM_{10} in the South Coast Air Basin of Southern California: part 1 – spatial variations. Journal of the Air and Waste Management Association 50 (12), 2034–2044.

Kim, H.S., Huh, J.B., Hopke, P.K., Holsen, T.M., Yi, S.M., 2007. Characteristics of the major chemical constituents of $PM_{2.5}$ and smog events in Seoul, Korea in 2003 and 2004. Atmospheric Environment 41 (32), 6762–6770.

Lee, J.H., Hopke, P.K., 2006. Apportioning sources of $PM_{2.5}$ in St. Louis, MO using speciation trends network data. Atmospheric Environment 40 (2), 360–377.

Lonati, G., Giugliano, M., Butelli, P., Romele, L., Tardivo, R., 2005. Major chemical components of $PM_{2.5}$ in Milan (Italy). Atmospheric Environment 39 (10), 1925–1934.

Louie, P.K.K., Watson, J.G., Chow, J.C., Chen, A., Sin, D.W.M., Lau, A.K.H., 2005. Seasonal characteristics and regional transport of $PM_{2.5}$ in Hong Kong. Atmospheric Environment 39 (9), 1695–1710.

Moller, D., 1990. The Na/Cl ration in rainwater and the seasalt chloride cycle. Tellus B 423, 254–262.

Miller, S.L., Anderson, M.J., Daly, E.P., Milford, J.B., 2002. Source apportionment of exposures to volatile organic compounds. I. Evaluation of receptor models using simulated exposure data. Atmospheric Environment 36 (22), 3629–3641.

National Bureau of Statistics of China, 2009. China Statistical Yearbook. China Statistics Press, Beijing (in Chinese).

Ocskay, R., Salma, I., Wang, W., Maenhaut, W., 2006. Characterization and diurnal variation of size-resolved inorganic water-soluble ions at a rural background site. Journal of Environmental Monitoring 8 (2), 300–306.

Park, S.S., Ondov, J.M., Harrison, D., Nair, N.P., 2005. Seasonal and shorter-term variations in particulate atmospheric nitrate in Baltimore. Atmospheric Environment 39 (11), 2011–2020.

Qin, Y.J., Kim, E., Hopke, P.K., 2006. The concentrations and sources of $PM_{2.5}$ in metropolitan New York City. Atmospheric Environment 40 (2), 312–332.

Querol, X., Alastuey, A., Moreno, T., Viana, M.M., Castillo, S., Pey, J., Rodríguez, S., Artiñano, B., Salvador, P., Sánchez, M., Garcia Dos Santos, S., Herce Garraleta, M.D., Fernandez-Patier, R., Moreno-Grau, S., Negral, L., Minguillón, M.C., Monfort, E., Sanz, M.J., Palomo-Marín, R., Pinilla-Gil, E., Cuevas, E., de la Rosa, J., Sánchez de la Campa, A., 2008. Spatial and temporal variations in airborne particulate matter (PM_{10} and $PM_{2.5}$) across Spain 1999–2005. Atmospheric Environment 42 (17), 3964–3979.

Salvador, P., Artíñano, B., Pio, C., Afonso, J., Legrand, M., Puxbaum, H., Hammer, S., 2010. Evaluation of aerosol sources at European high altitude background sites with trajectory statistical methods. Atmospheric Environment 44 (19), 2316–2329.

Seinfeld, J.H., 1986. Atmospheric Chemistry and Physics of Air Pollution. Wiley, New York.

Shen, Z.X., Cao, J.J., Arimoto, R., Han, Z.W., Zhang, R.J., Han, Y.M., Liu, S.X., Okuda, T., Nakao, S., Tanaka, S., 2009. Ionic composition of TSP and $PM_{2.5}$ during dust storms and air pollution episodes at Xi'an, China. Atmospheric Environment 43 (18), 2911–2918.

Shou, Y.P., Gao, X.M., Wang, J., Yang, L.X., Wang, W.X., 2010. Online measurement of water-soluble ions in fine particles from the atmosphere in autumn in Jinan. Research of Environmental Sciences 23 (1), 41–47.

Sloane, C.S., Watson, J., Chow, J., Pritchett, L., Richards, L.W., 1991. Size-segregated fine particle measurements by chemical species and their impact on visibility impairment in Denver. Atmospheric Environment. Part A. General Topics 25 (5–6), 1013–1024.

Stohl, A., 1996. Trajectory statistics-a new method to establish source-receptor relationships of air pollutants and its application to the transport of particulate sulfate in Europe. Atmospheric Environment 30 (4), 579–587.

Streets, D.G., Fu, J.S., Jang, C.J., Hao, J.M., He, K.B., Tang, X.Y., Zhang, Y.H., Wang, Z.F., Li, Z.P., Zhang, Q., Wang, L.T., Wang, B.Y., Yu, C., 2007. Air quality during the 2008 Beijing Olympic Games. Atmospheric Environment 41 (3), 480–492.

Sun, Y.L., Zhuang, G.S., Tang, A.H., Wang, Y., An, Z.S., 2006. Chemical characteristics of $PM_{2.5}$ and PM_{10} in haze-fog episodes in Beijing. Environmental Science & Technology 40 (10), 3148–3155.

Wang, T., Nie, W., Gao, J., Xue, L.K., Gao, X.M., Wang, X.F., Qiu, J., Poon, C.N., Meinardi, S., Blake, D., Wang, S.L., Ding, A.J., Chai, F.H., Zhang, Q.Z., Wang, W.X., 2010. Air quality during the 2008 Beijing Olympics: secondary pollutants and regional impact. Atmospheric Chemistry and Physics 10, 7603–7615.

Wang, Y., Zhuang, G.S., Tang, A.H., Yuan, H., Sun, Y.L., Chen, S., Zheng, A.H., 2005. The ion chemistry and the source of $PM_{2.5}$ aerosol in Beijing. Atmospheric Environment 39 (21), 3771–3784.

Wang, Y., Zhuang, G.S., Zhang, X.Y., Huang, K., Xu, C., Tang, A.H., Chen, J.M., An, Z.S., 2006. The ion chemistry, seasonal cycle, and sources of $PM_{2.5}$ and TSP aerosol in Shanghai. Atmospheric Environment 40 (16), 2935–2952.

Westberg, H.M., Byström, M., Leckner, B., 2003. Distribution of potassium, chlorine, and sulfur between solid and vapor phases during combustion of wood chips and coal. Energy & Fuels 17 (1), 18–28.

Wu, W.S., Wang, T., 2007. On the performance of a semi-continuous $PM_{2.5}$ sulphate and nitrate instrument under high loadings of particulate and sulphur dioxide. Atmospheric Environment 41 (26), 5442–5451.

Wu, Z.J., Hu, M., Shao, K.S., Slanina, J., 2009. Acidic gases, NH_3 and secondary inorganic ions in PM_{10} during summertime in Beijing, China and their relation to air mass history. Chemosphere 76 (8), 1028–1035.

Xu, J., Bergin, M.H., Yu, X., Liu, G., Zhao, J., Carrico, C.M., Baumann, K., 2002. Measurement of aerosol chemical, physical and radiative properties in the Yangtze delta region of China. Atmospheric Environment 36 (2), 161–173.

Xu, P.J., Wang, W.X., Yang, L.X., Zhang, Q.Z., Gao, R., Wang, X.F., Nie, W., Gao, X.M., 2010. Aerosol size distributions in urban Jinan: seasonal characteristics and variations between weekdays and weekends in a heavily polluted atmosphere. Environmental Monitoring and Assessment. doi:10.1007/s10661-010-1747-2.

Yang, L.X., Wang, D.C., Cheng, S.H., Wang, Z., Zhou, Y., Zhou, X.H., Wang, W.X., 2007. Influence of meteorological conditions and particulate matter on visual range impairment in Jinan, China. Science of Total Environment 383 (1–3), 164–173.

Yao, X.H., Chan, C.K., Fang, M., Cadle, S., Chan, T., Mulawa, P., He, K.B., Ye, B., 2002. The water-soluble ionic composition of $PM_{2.5}$ in Shanghai and Beijing, China. Atmospheric Environment 36 (26), 4223–4234.

Zhang, K., Wang, Y.S., Wen, T.X., Liu, G.R., Xu, H.H., 2007a. On-line analysis the water-soluble chemical of $PM_{2.5}$ in late summer and early autumn in Beijing. Acta Scientiae Circumstantiae 27 (3), 459–465.

Zhang, Q., Jimenez, J.L., Canagaratna, M.R., Allan, J.D., Coe, H., Ulbrich, I., Alfarra, M.R., Takami, A., Middlebrook, A.M., Sun, Y.L., Dzepina, K., Dunlea, E., Docherty, K., DeCarlo, P.F., Salcedo, D., Onasch, T., Jayne, J.T., Miyoshi, T., Shimono, A., Hatakeyama, S., Takegawa, N., Kondo, Y., Schneider, J., Drewnick, F., Borrmann, S., Weimer, S., Demerjian, K., Williams, P., Bower, K., Bahreini, R., Cottrell, L., Griffin, R.J., Rautiainen, J., Sun, J.Y., Zhang, Y.M., Worsnop, D.R., 2007b. Ubiquity and dominance of oxygenated species in organic aerosols in anthropogenically-influenced Northern Hemisphere midlatitudes. Geophysical Research Letters 34, L13801. doi:10.1029/2007GL029979.

Zhang, Q., Streets, D.G., Carmichael, G.R., He, K.B., Huo, H., Kannari, A., Klimont, Z., Park, I.S., Reddy, S., Fu, J.S., Chen, D., Duan, L., Lei, Y., Wang, L.T., Yao, Z.L., 2009. Asian emissions in 2006 for the NASA INTEX-B mission. Atmospheric Chemistry and Physics 9, 5131–5153.

Zhou, X.H., Cao, J., Wang, T., Wu, W.S., Wang, W.X., 2009. Measurement of black carbon aerosols near two Chinese megacities and the implications for improving emission inventories. Atmospheric Environment 43 (25), 3918–3924.

Zhou, Y., Wang, T., Gao, X.M., Xue, L.K., Wang, X.F., Wang, Z., Gao, J., Zhang, Q.Z., Wang, W.X., 2010. Continuous observations of water-soluble ions in $PM_{2.5}$ at Mount Tai (1534 ma.s.l.) in central-eastern China. Journal of Atmospheric Chemistry. doi:10.1007/s10874-010-9172-z.